

# Analysis of The Etching Mechanisms of Tungsten in Fluorine Containing Plasmas

Patrick Verdonck

LSI PEE EPUSP, Sao Paulo, Brazil

Jacobus Swart\*

DSIF FEE UNICAMP, Campinas, Brazil

Guy Brasseur

Cobrain N.V., 3001 Leuven, Belgium

Pascal De Geyter

IMEC v.z.w. , 3001 Leuven, Belgium

## ABSTRACT

Tungsten and polysilicon layers were etched in three different types of etching equipment, in different etching modes. Etch rates and wall profiles were determined. Partially etched tungsten layers were analyzed through Auger spectroscopy. Combining all these results, it was possible to determine the etch rate limiting subprocesses for tungsten etching. For most process conditions, the arrival of atomic fluorine at the wafer surface is the etch rate limiting mechanism. For other processes, the removal of products with low volatility is the limiting mechanism.

## Introduction

Tungsten and tungsten silicide are becoming increasingly important materials for the fabrication of integrated circuits. Tungsten is used as a material for plug formation,<sup>1</sup> interconnect material,<sup>2</sup> gate material, mainly for self-aligned metal semiconductor field effect transistors (MESFETs),<sup>3</sup> and as absorber material in x-ray masks.<sup>4</sup>

Etching mechanisms have been reported in the literature, but to a much lesser extent than for silicon.<sup>5-10</sup> These mechanisms are still not well understood and remain controversial.

The influence of oxygen addition to SF<sub>6</sub> and CF<sub>4</sub> has been studied intensively. At low oxygen concentrations, the fluorine concentration, as determined by actinometric measurements and silicon and tungsten etch rates, increases with the oxygen concentration. By increasing the oxygen concentration further, first the silicon etch rate starts to decrease, then the fluorine concentration, and at last the tungsten etch rate.<sup>5-7</sup>

From these results, mass spectroscopy and x-ray photoelectron spectroscopy (XPS) analysis the following model has been proposed.<sup>5,8,9</sup> There are three regions of oxygen concentration where the dominant etch mechanisms are different. In the first region, at a low oxygen concentration, the etch rate is determined by the F content, and WF<sub>6</sub> is formed. At intermediate oxygen concentrations the formation of WOF<sub>4</sub> helps to keep the etch rate high, although WOF<sub>4</sub> is less volatile than WF<sub>6</sub>. When more oxygen is added there is competition in the formation of tungsten fluorides and tungsten oxides<sup>5</sup> or the dilution is too large to generate enough free fluorine to form one of the halogenated volatile etch products and therefore the tungsten etch rate decreases.

The maximum silicon etch rate is located at lower oxygen flows than the maximum of the free fluorine concentration. This is caused by the competition between O and F atoms to form bonds with Si. The SiOF<sub>2</sub> and SiO<sub>2</sub> product molecules are not volatile and therefore decrease the etch rate.

Ion bombardment can be a very important etch rate factor for increasing tungsten etching. Ion bombardment caused by electrostatic potentials as small as 25 V, increases the etch rate by a factor of two.<sup>6</sup>

Reports on the anisotropy of the tungsten etch processes show a multiplicity of results.<sup>6,7,10</sup> Some reports assume that a polymer has to be formed to protect sidewall etching. Other reports state that the formation of active W sites through ion bombardment increases the vertical to horizontal etch rate so that anisotropy is obtained.

The characteristics of purely chemical etching, *i.e.*, without any ion bombardment vary widely. Fracassi *et al.* report an extremely low etch rate when no ion bombardment is present.<sup>6</sup> Hess also reports very low etch rates in the plasma etch (PE) mode.<sup>5</sup> Daubenspeck *et al.* show etch rates in the PE mode as high as in reactive ion etch (RIE) mode.<sup>11</sup> In this case the model of associative desorption describes well the chemical reactions which occur at the surface of the tungsten layer.<sup>12</sup>

In this paper we shall show that there are several etch rate limiting mechanisms, that ion bombardment is important, but that chemical etching without ion bombardment can yield high etch rates, dependent on process parameters.

## Experimental

Samples are prepared as follows: <100> silicon wafers of 125 mm diam first receive a 500 nm thick film of plasma-enhanced chemical vapor deposition (PECVD) oxide. Then

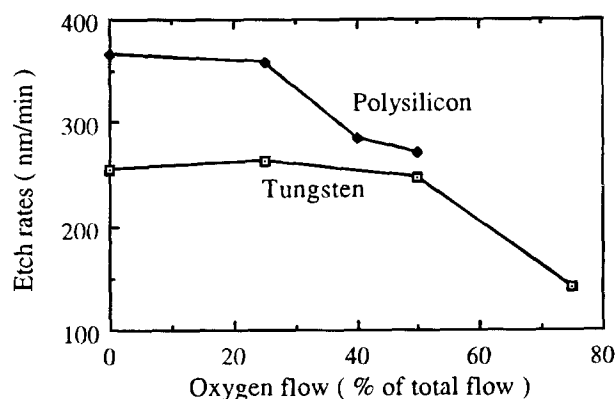


Fig. 1. Tungsten and polysilicon etch rates as a function of oxygen flow, for NF<sub>3</sub>-O<sub>2</sub> plasmas in the RIE mode, at 150 Torr pressure, and 50 W power in the SWAFER reactor.

\* Electrochemical Society Active Member.

**Table I. Tungsten etch rates, uniformities, and selectivities toward resist as a function of pressure and power in the SWAFER reactor in RIE mode.**

NF <sub>3</sub> flow (sccm)	Pressure (mTorr)	Power (W)	Etch rate (nm/min)	Uniformity (%)	Selectivity W/resist
125	150	50	206	±7	0.86
125	150	100	330	±6	0.67
125	150	150	410	±5	0.41
62	75	50	156	±6	0.62
31	40	50	110	±2	0.58
62	75	100	252	±6	0.38

a barrier layer (TiW or TiN) is deposited followed by a 1 μm CVD tungsten deposition. Patterning (with both light field and dark field masks) is performed with a stepper, with the possibility of different step patterns, using the Shipley 1713 resist. On some samples, 500 nm of PECVD oxide are deposited on top of the tungsten layer. On top of this oxide, Shipley 1713 resist is patterned. The oxide is then plasma etched in order to be used as a mask during the tungsten etching.

Three different etching equipment are used.

1. *A Cobrain swafer*.—Power, at 25 kHz frequency, is applied at the lower electrode leaving the upper electrode grounded in the RIE mode, or at the upper electrode leaving the lower electrode floating in a PE mode.<sup>13</sup>

2. *A Tegal HRe-system*.—Permanent magnets are placed around the cylindrical wall and above the upper electrode. The upper electrode is always grounded. It is possible to apply power at 13.56 MHz at the wall of the reactor (PE mode) or at the lower electrode (RIE mode).<sup>14</sup>

3. *A few experiments were performed using MATRIX 303 equipment*.—A remote plasma is created in the upper part of the reactor, while the wafer is placed in the lower part, on a heated chuck. Both parts of the reactor are divided by a grid made of alumina.

## Results and Discussion

*Etching Behavior*.—First, etch rates, uniformities, selectivities, and wall profiles for NF<sub>3</sub> containing plasmas were investigated in the SWAFER, in both the RIE and PE mode.

The etch rates of silicon and tungsten in the RIE mode as a function of oxygen content are shown in Fig. 1. Total flow was 100 sccm, pressure was 150 mTorr, and power was 50 W.

This figure shows that the etch rates do not increase much with the addition of oxygen, which is different from the results in Ref. 5-7. The binding energies between S and F atoms in SF<sub>6</sub> or C and F atoms in CF<sub>4</sub> are higher than the binding energies between the N and the F atoms in NF<sub>3</sub>.<sup>15</sup> Therefore for NF<sub>3</sub>, the addition of oxygen does not increase, as much, the formation of free fluorine as in the cases of SF<sub>6</sub> or CF<sub>4</sub>. Extra tests using SF<sub>6</sub> + O<sub>2</sub> show results similar to the ones reported in Ref. 5-7. For oxygen flows of over 25% of the total flow, the silicon etch rate starts to decrease, as expected. The tungsten etch rate starts to decrease at 50% of oxygen flow, probably due to dilution.

Table I shows tungsten etch rates, uniformities, and selectivities of tungsten toward the resists as a function of power and pressure.

Etch rates increase with power but much less than proportionately. An increase of power does not increase very much the formation of free fluorine in this etching mode, at these power levels. This phenomenon agrees with the fact that the addition of oxygen does not increase the etch rate nor the fluorine atom concentration.

The uniformities of the etch rates of RIE processes are good. When measuring the inner 110 mm of a 125 mm wafer with an automatic spreading resistance probe, uniformities are typically ±6%. At lower pressures the uniformity im-

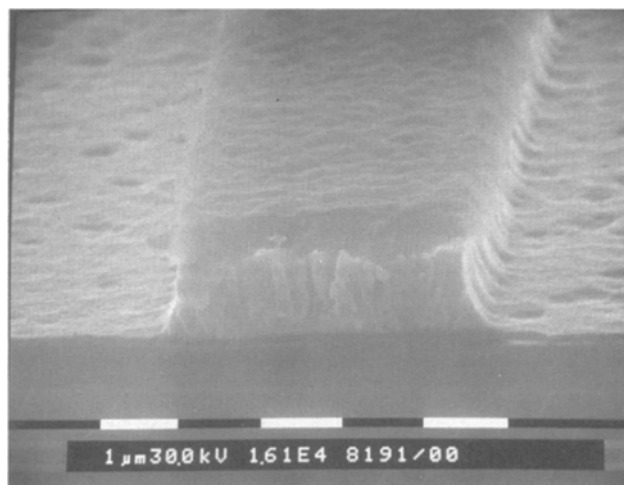


**Fig. 2. Tungsten profile after RIE etching with a pure NF<sub>3</sub> plasma using a PECVD oxide mask.**

proves, obtaining ±4% for a 75 mTorr process. This improvement in uniformity can be explained through the increase of the diffusion coefficient of gases at lower pressures.<sup>16</sup>

Selectivities towards resist are rather low. For the zero oxygen flow process, the selectivity of tungsten to resist is of the order of 0.9. Selectivities increase with pressure and decrease with power.

Two types of masks were used to investigate the wall profile: a standard resist mask and a PECVD oxide mask.

When using a resist mask, the wall profile was vertical for all the processes performed in the RIE mode, never was any undercutting observed. When using a PECVD mask, the wall profile remains vertical, but there is a very slight undercutting, as shown in Fig. 2. This indicates that in this etching mode, the ion bombardment enhanced etching is predominant, but there also exists a slight chemical etching. The fact that with a PECVD oxide mask almost no undercutting occurs using a NF<sub>3</sub> + O<sub>2</sub> gas mixture, suggests that no polymerization is needed to obtain a vertical wall. In this etching mode, the ion bombardment does increase the etch rate considerably.

The etch rates of silicon and tungsten in the PE mode as a function of oxygen content are shown in Fig. 3. Total flow was 75 sccm, pressure was 200 mTorr, and the power was 50 W. This figure shows that the etch rates increase as expected with the addition of oxygen. The fact that the etch rate of tungsten starts to decrease at a lower oxygen content than the etch rate of silicon is rather unexpected and is commented on below.

Table II shows tungsten etch rates and uniformities as a function of power in the PE mode.

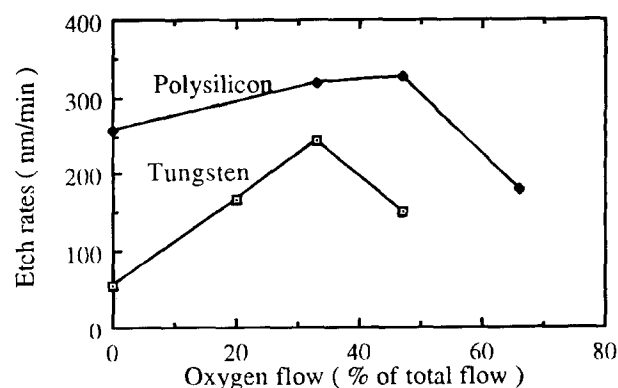


**Fig. 3. Tungsten and polysilicon etch rates as a function of oxygen flow, for NF<sub>3</sub>-O<sub>2</sub> plasmas in PE mode, at 150 mTorr pressure and 50 W power in the SWAFER reactor.**

**Table II. Tungsten etch rates and uniformities as a function of power in the SWAFER reactor in PE mode.**

NF <sub>3</sub> flow (sccm)	O <sub>2</sub> flow (sccm)	Power (W)	Etch rate (nm/min)	Uniformity (%)
105	20	150	375	±13
105	20	100	302	±12
105	20	75	230	±11
105	20	50	165	±10

For NF<sub>3</sub> plasmas containing O<sub>2</sub>, tungsten etch rates do increase with power from 50 to 100 W proportionately, but from then on less than proportionately.

Both these phenomena indicate that in this etching mode at 50 W, more free fluorine can easily be formed by increasing the power or by adding some oxygen.

The tungsten etch rate is dependent on the resist coverage. The inverse of the traditional loading effect is observed: for dark field masked wafers (95% resist coverage) the etch rate can be 50% lower than the etch rate of light-field masked wafers (5% resist coverage). Blanket tungsten-covered wafers etch even faster. When the mask is made of PECVD oxide, the etch rate of tungsten increases with coverage: layers with 95% coverage etch up to twice as fast as the blanket tungsten layers. In this case the traditional loading effect occurs. Polysilicon layers also etch faster when less free area is available, even when the mask consists of a resist.

The type of nonuniformity also depends on the resist coverage. Blanket tungsten layers and layers covered with a PECVD oxide mask always etch faster at the border of the wafer than in the center, as is also the case for all polysilicon layers. Resist covered tungsten layers also etch faster at the border than in the center if an edge-bead removal has been performed. On the other hand, if the outer 5 mm of the wafer is covered with resist, the tungsten etch rate is higher in the center than at the border. This is shown in Fig. 4. It shows the etch rates for a wafer which had no edge-bead removal and for a wafer where the outer 5 mm of resist (the edge-bead) were removed, as a function of the radial position on the wafer.

The influence of the resist coverage could be observed in still another way. At approximately 30 mm from the border, a resist area of approximately 2 cm<sup>2</sup> was left unpatterned. When etching completely through the tungsten and in the underlying PECVD oxide, it was possible to measure the remaining thickness of this oxide. Figure 5 shows the result. The fact that at 2 mm from this area, the PECVD layer is thicker, indicating that the tungsten etch rate is locally lower than farther away from the large resist area. (Other tests showed that the silicon dioxide etch rate is not dependent on resist coverage.)

Spaces of 1 μm width etch at the same rate as spaces of 20 μm width, just as there is no difference in the etch rates

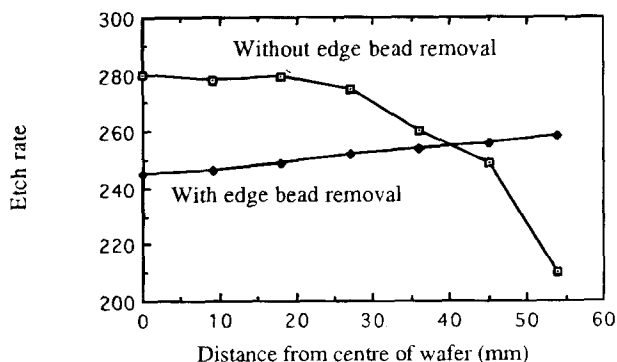


**Fig. 4. Tungsten etch rates as a function of position on the wafer, for a wafer with edge-bead removal and a wafer without edge-bead removal. Process: 100 sccm of NF<sub>3</sub>-20 sccm of O<sub>2</sub>, in PE mode, at 150 mTorr pressure and 50 W power in the SWAFER reactor.**

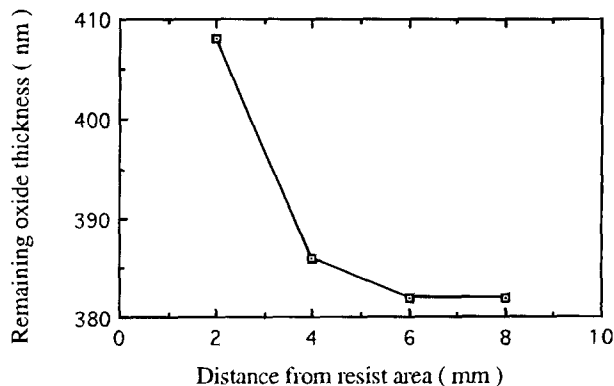


**Fig. 5. Remaining PECVD oxide thickness as a function of distance from a large resist area after a PE mode etching with a NF<sub>3</sub>-O<sub>2</sub> plasma in the SWAFER reactor.**

of spaces between 1 μm wide resist lines and 20 μm resist lines. This suggests that the etch rate limiting effect of the resist is rather a long range (macro-) than a short range (micro-) phenomenon.

It has been reported<sup>17,18</sup> that an oxidation of the tungsten surface occurs when a tungsten layer which was partially etched in the PE mode, is exposed to air. The proposed mechanism is that fluorine diffuses into the tungsten layer during the etching in the PE mode (typically as far as 15 nm under the surface) and forms W-F bonds. When exposed to air, the fluorine is substituted by oxygen atoms, forming W-O bonds. When applying a short RIE plasma before the wafer leaves the reactor, no oxide is formed in the air. This indicates that the W-F layer is completely removed in a RIE plasma.

Through Auger analysis, it is possible to determine that at 2 mm from the large resist area, the oxygen was found to be 70% deeper than at 6 mm from this large resist area. Therefore one can conclude that more F was able to diffuse deeper into the tungsten near the resist. We conclude that lack of fluorine is therefore not the reason of the lower etch rate near the resist.

Besides, resist etch rates are very low in the PE mode, typically 10 nm/min, therefore it is not resist erosion which consumes the atomic fluorine and would cause, in this way, a decrease in tungsten etch rate. A possible explanation for these phenomena is presented below.

In this etching mode (PE), two types of masks were used to investigate the wall profile: a standard resist mask and a PECVD oxide mask. Severe undercutting is consistently observed, whatever the type of mask used, as shown in Fig. 6. This indicates that etching is isotropic (and therefore chemical).

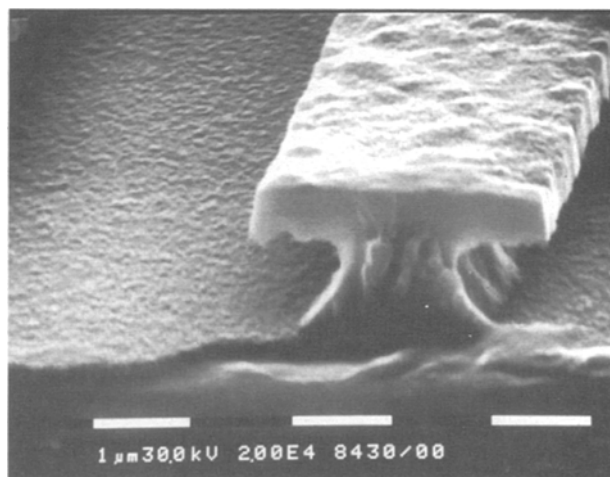


**Fig. 6. Tungsten profile after PE mode etching with a NF<sub>3</sub>-O<sub>2</sub> plasma, using a PECVD oxide mask.**

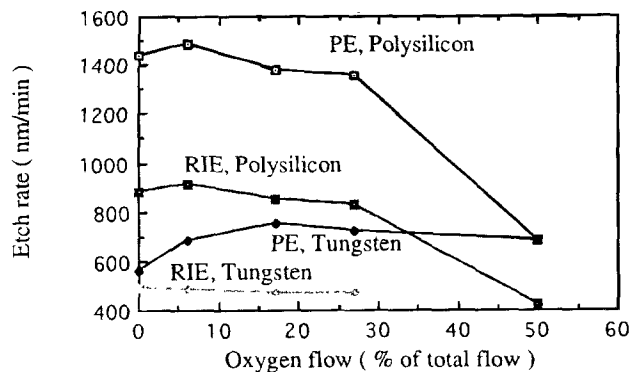


Fig. 7. Tungsten and polysilicon etch rates as a function of oxygen flow and etching mode. Total flow, 96 sccm; pressure, 10 mTorr; power, 400 W in the TEGAL HRE-reactor.

Etching of tungsten is also investigated with Matrix 303 equipment, using  $\text{NF}_3$  gas. In this system we are able to etch tungsten, albeit rather slowly, and we also observe the same formation of tungsten oxide, once a partially etched wafer is exposed to air. This shows that chemical etching is possible and that formation of tungsten oxide is a general phenomenon, not just one related to the SWAFER.

Etch rates, uniformities, selectivities, and wall profiles for  $\text{SF}_6$  containing plasmas are investigated in the Tegal HRE-, both in PE and RIE mode.<sup>18,19</sup>

The etch rates of silicon and tungsten as a function of oxygen flow are shown in Fig. 7 for both the PE and the RIE mode. Total flow was 96 sccm, pressure 10 mTorr, and power 400 W.

This figure shows that the etch rates do not increase much with the addition of oxygen, except for the tungsten in the PE mode. For oxygen flows of over 26% the silicon etch rate starts to decrease, as expected.

Etch rates do increase with power but only very little, what indicates that there is already quite a high concentration of fluorine atoms at this power level.

Actinometric measurements also show that fluorine concentration does not increase with power (at this power level) and oxygen addition.<sup>18</sup> These facts can be explained by the high efficiency of the magnetically confined plasma. The very high etch rates indicate that a large amount of atomic fluorine is formed, in both the PE and the RIE mode.

In the RIE mode, uniformities are very good. For example, when measuring within a diameter of 110 mm with an automatic spreading resistance probe, the uniformities are typically  $\pm 3\%$ . The lower the pressure, the better the uniformity. This behavior is also observed for the PE mode, though in this mode uniformities are much poorer,  $\pm 10\%$  typically.

Selectivities toward the resist are rather low. For the zero oxygen flow process, the selectivity ratio of tungsten to resist is of the order of 1:1 in the RIE mode. In the PE mode the selectivity ratios are higher, of the order of 5:1.

In the RIE mode no undercutting was observed using resist masks, as in the RIE mode for the SWAFER. In the PE mode, the etching was isotropic, as in the PE mode for the SWAFER. No oxidation of the tungsten was found after etching in this system.

**Etch rate limiting steps.**—In the Appendix, we show that it is possible to calculate the fluorine consumption,  $J_F$ , during etching of a (bare) wafer by the following formula

$$J_F = 2.24 \cdot 10^{-3} \cdot A \cdot r \cdot \rho \cdot x/M \quad [1]$$

where

$J_F$  = flow of atoms consumed in sccm

$A$  = free area of the wafer in  $\text{cm}^2$

$r$  = etch rate of the film in  $\text{nm}/\text{min}$

$\rho$  = density of the film material in  $\text{kg}/\text{dm}^3$

$x$  = coefficient of the overall reaction,

$\text{Mat} + x \text{F} \rightarrow \text{MatF}_x$

$M$  = atomic weight of the film material in  $\text{g}/\text{mol}$

The value for the free area depends on the resist coverage. For our purposes we assumed that the resist did not consume any fluorine, as the resist coverage was always less than 5%.

By comparing the flow of consumed fluorine during the tungsten etching with the flow during the silicon etching, it is possible to draw conclusions on the rate limiting mechanism. If the rate limiting step is the arrival of free fluorine on the wafer, the fluorine consumption of both etchings should be approximately the same, as the generation of the fluorine atoms will be slightly influenced by the film to be etched and not at all by the diffusion of the species toward the film. If other mechanisms, such as chemisorption or removal of the volatile product, become the etch rate limiting step, it is very improbable that the fluorine consumption will be the same for both materials, as these mechanisms are considerably more material dependent.

The consumed fluorine flow was calculated through reaction 1 for the tungsten and silicon etching processes as shown before. This results in Fig. 8 for the case of the SWAFER.

In the RIE mode, the fluorine consumption is approximately the same for Si and W in the region from 0 to 25% of oxygen flow. This indicates that in this region the arrival of free fluorine is the etch rate limiting step. For higher oxygen flows, the consumption is lower for the polysilicon than for the tungsten. This can be explained by the formation of the nonvolatile  $\text{SiO}_2$  and  $\text{SiOF}_2$  molecules in the case of the silicon, while  $\text{WOF}_4$  is sufficiently volatile to be removed in this etching mode.

In the PE mode, the fluorine consumption is the same for both materials only in a small flow range, around 30% of the oxygen flow. Out of this range the fluorine consumption is always lower for tungsten. This means that in those areas other mechanisms control the etch rate.

For the higher oxygen flow range we propose the following mechanism. It is common to assume the formation of  $\text{WOF}_4$  as a volatile etch product, as mentioned in the introduction. The boiling point of  $\text{WOF}_4$  is  $188^\circ\text{C}$ . Most papers in the literature treat RIE or RIE-like plasmas, which occur with a considerable amount of ion bombardment. In the PE mode, however, very little ion bombardment occurs. We propose that in this mode, it is much harder to remove  $\text{WOF}_4$  than in the RIE mode. Therefore, formation of  $\text{WOF}_4$  results in decreasing the etch rate instead of increasing it. This hypothesis is compatible with results from other authors in completely different process conditions.<sup>20</sup> One should observe that in the  $\text{WOF}_4$  molecule only one O atom per four F atoms is needed, while for the  $\text{SiOF}_2$  one O atom per two F atoms is needed. Therefore, it is normal that  $\text{WOF}_4$  is formed in larger quantities at lower oxygen flows than  $\text{SiOF}_2$ . In this way one can explain that the etch rate of tungsten decreases at a lower oxygen flow than that of silicon.

For the lower oxygen flow range, we propose a mechanism which inhibits the tungsten etching, caused by the interaction with the resist, as is explained below.

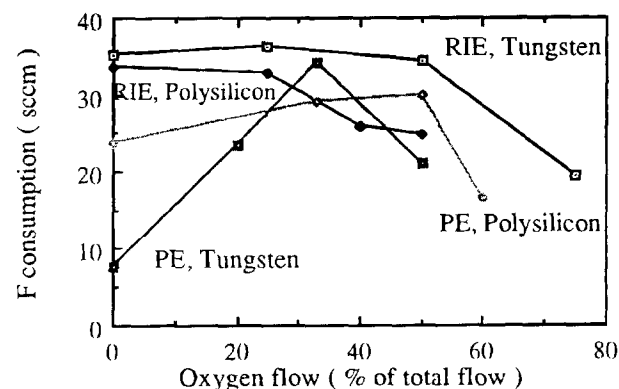


Fig. 8. Fluorine consumption for tungsten and polysilicon etch processes as a function of oxygen flow and etching mode in the SWAFER.

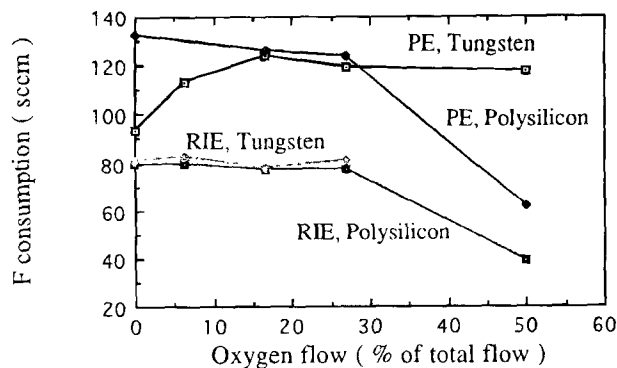


Fig. 9. Fluorine consumption for tungsten and polysilicon etch processes as a function of oxygen flow and etching mode in the Tegal HRE.

Figure 9 shows the fluorine consumption in the Tegal HRE for silicon and tungsten etching in both the PE and the RIE mode.

In the RIE mode the fluorine consumption is the same for the measured range, indicating that the rate is really limited by the arrival of the fluorine atoms.

In the PE mode the fluorine consumption is the same in the 20 to 30% oxygen flow range.

For the higher oxygen flows, consumption is higher for tungsten, contrary to the case of etching in the PE mode in the SWAFER. This can be explained by the traditional formation of  $\text{SiO}_2$ ,  $\text{SiOF}_2$ , and  $\text{WOF}_4$ , with  $\text{WOF}_4$  being volatilized by ion bombardment, present in the HRE-, even in the PE mode.

For no oxygen flow, the consumption is lower for the tungsten. This is just the same as for the PE mode in the SWAFER. It seems that a similar mechanism occurs for this kind of etching mode in both sets of equipment.

The fact that the silicon consumption for the silicon etching is higher than for the tungsten etching means that the tungsten etch rate is not limited by the arrival of fluorine atoms. From the tests in the SWAFER we also know that the presence of resist decreases the etch rates of tungsten in PE mode. In the neighborhood of large resist areas, the tungsten etch rate also decreases, as indicated by Fig. 5. From Auger analyses in the neighborhood of this area, we know that the decrease of etch rate is not due to the lack of fluorine atoms, as mentioned before. Therefore, also in this area, another etch rate limiting mechanism must occur. It is this same mechanism, which causes resist covered tungsten layers to etch more slowly than blanket tungsten layers in the PE mode in the SWAFER.

The fact that after a short RIE-type plasma, no oxidized layer is formed, indicates that fluorine atoms are only diffusing into the tungsten when (little or) no ion bombardment is available. During ion bombardment assisted etching, the etching occurs so rapidly that no fluorine can diffuse into the tungsten.

We conclude that the constituents of the resist, typically carbon, combine with tungsten and/or fluorine to form a compound on the surface which inhibits the etching, if it is not removed by ion bombardment, as in the case of the RIE mode, or by etching by the oxygen, as is the case for the processes with higher oxygen flows. This phenomenon is not particular to one type of equipment, but rather to a certain etching mode, in which chemical etching prevails over ion bombardment enhanced etching.

### Conclusion

The experimental results and its analyses lead to the following conclusions.

1. For most process conditions, the flow of fluorine atoms arriving at the tungsten surface is the etch rate limiting mechanism.

2. When adding oxygen to the halogen,  $\text{WOF}_4$  is formed as an etch product. It contributes to sustain the tungsten

etch rate if enough ion bombardment occurs. For process conditions with little or no ion bombardment,  $\text{WOF}_4$  decreases the etch rate.

3. For some process conditions, the interaction plasma resist tungsten surface forms an etch rate decreasing layer. This layer can be completely removed if enough oxygen and/or ion bombardment is available. The presence of large resist areas helps in the formation of this layer and can cause a local decrease of tungsten etch rates.

4. In plasmas with high concentration of free fluorine and low ion bombardment, fluorine diffuses into the upper layers of the tungsten film. When this fluorinated layer is exposed to air, it forms an oxidized layer.

5. Ion bombardment in general enhances the tungsten etch rate and if enough bombardment is available, anisotropic etching occurs.

6. When enough free fluorine is generated, pure chemical etching is possible (even without any ion bombardment).

### Acknowledgments

The authors thank Dr. Hugo Bender for the Auger analyses and helpful discussions and Professor Dr. Jorge Santiago-Aviles for discussions and encouragement.

Manuscript submitted Nov. 3, 1994; revised manuscript received Feb. 7, 1995. This was in part Paper 236 presented at the San Francisco, CA, Meeting of the Society, May 22-27, 1994.

LSI PEE EPUSP, DSIF-Unicamp, Cobrain, and IMEC assisted in meeting the publication costs of this article.

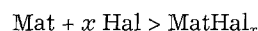
### APPENDIX

It is possible to calculate the consumption of the etch reactant by making a few assumptions:

A 1 nm thick film has a weight of:  $A \cdot r \cdot 10^{-7}$  g where  $A$  is the area of the wafer in  $\text{cm}^2$  and  $\rho$  is the density of the film material in  $\text{g}/\text{cm}^3$ .

Knowing the atomic weight of the material, one can calculate the number of moles in this 1 nm thick sheet by  $A \cdot \rho \cdot 10^{-7}/M$  mol where  $M$  is the atomic weight of the film material in  $\text{g}/\text{mol}$ .

Assuming that the only etch reaction of the material, Mat, with the halogen species, Hal, is the following



then the consumption of halogen species in moles to remove a 1 nm thick layer is  $A \cdot \rho \cdot 10^{-7} \cdot x/M$  mol.

If the material is removed with an etch rate  $r$  in  $\text{nm}/\text{min}$ , the consumption of halogen species in  $\text{mol}/\text{min}$  is

$$A \cdot r \cdot \rho \cdot 10^{-7} \cdot x/M \text{ mol}/\text{min}$$

One mole of gas occupies  $22,400 \text{ cm}^3$  under standard conditions of pressure and temperature. To calculate the flow of consumed halogen species,  $J_{\text{HAL}}$ , in  $\text{sccm}$ , the following formula has to be applied

$$J_{\text{Hal}} = 2.24 \cdot 10^{-3} A \cdot r \cdot \rho \cdot x/M \text{ sccm}$$

### REFERENCES

1. P. Reily and T. Clark, *This Journal*, **138**, 3008 (1991).
2. Y. Pauleau, *Solid State Technol.*, **30**, 61 (1987).
3. N. Yamamoto, H. Kume, S. Iwata, K. Yagi, N. Kobayashi, N. Mori, and H. Miyazaki, *This Journal*, **133**, 401 (1986).
4. C. Jurgensen, R. Kola, A. Novembre, W. Tai, J. Frackoviak, L. Trimble, and G. Celler, *J. Vac. Sci. Technol.*, **B9**, 3280 (1991).
5. D. Hess, *Solid State Technol.*, **31**, 97 (1988).
6. F. Fracassi and J. Coburn, *J. Appl. Phys.*, **63**, 1758 (1988).
7. J. M. Collumeau, J. Etrillard, J. F. Bresse, and C. Dubon-Chevalier, *This Journal*, **137**, 671 (1990).
8. K. Greenberg and T. Verdeyen, *J. Appl. Phys.*, **57**, 1596 (1985).
9. R. Petri, D. Henry, and N. Sadeghi, *J. Appl. Phys.*, **72**, 2644 (1992).
10. T. Whetten, N. Whetten, and E. Wolf, in *Tungsten and Other Refractory Metals for VLSI Applications-II*,

- R. S. Blewer and C. M. McConica, Editors, MRS Pittsburgh, PA (1987).
11. T. Daubenspeck and P. Sukanek, *This Journal*, **136**, 3779 (1989).
  12. A. Durandet, Y. Arnal, J. Pelletier, and G. Pomot, *J. Appl. Phys.*, **67**, 2298 (1990).
  13. G. Brasseur, P. Bruneel, C. Jehoul, and J. Vandersmissen, in *Proceedings of Microcircuit Engineering 90*, F. Coopmans, L. Van den hove (1990).
  14. P. Laporte, L. Van den hove, and Y. Melaku, *SPIE Proc.*, **1392**, J. Bondur and T. R. Turner, p. 196, SPIE (1990).
  15. *CRC Handbook of Chemistry and Physics*, 65th ed., R. Weast, Editor, CRC Press, Inc., Bacon Raton, FL (1984-1985).
  16. R. Reid and T. Sherwood, *The Properties of Gases and Liquids*, 2nd ed., McGraw Hill, Inc., New York (1986).
  17. P. Verdonck, G. Brasseur, and J. Swart, in *Proceedings of Microcircuit Engineering-21*, p. 329, Elsevier, New York (1993).
  18. P. Verdonck, Ph.D. Thesis, Unicamp, Campinas Brazil (1993).
  19. P. De Geyter, M. Lux, P. Verdonck, L. Van den hove, and T. B. Pham, in *Proceedings of the Tegal European Plasma Seminar 1993*.
  20. J. F. Coulon and G. Turban, *Mater. Sci. Eng.*, **A 139**, 385 (1991).

# Deposition Mechanism of Silicon Nitride in Direct Photoassisted Chemical Vapor Deposition Using a Low-Pressure Hg Lamp

Masahiro Yoshimoto, Kenji Takubo,<sup>a</sup> Tetsuya Ohtsuki,<sup>b</sup> Michio Komoda,<sup>c</sup> and Hiroyuki Matsunami

Department of Electrical Engineering, Kyoto University, Sakyo, Kyoto 606-01, Japan

## ABSTRACT

Silicon nitride ( $\text{SiN}_x$ ) films applicable to microelectronics are deposited by photoassisted chemical vapor deposition (CVD) with a low-pressure Hg lamp (185 nm). We describe the deposition mechanism of  $\text{SiN}_x$  in the photo-CVD based on analyses of film structures and transient mass spectroscopy.  $\text{NH}_3$  is decomposed into  $\text{NH}_2$  and H by UV-light irradiation.  $\text{SiH}_4$  is decomposed through the reaction with  $\text{NH}_2$  or H.  $\text{SiN}_x$  films are formed through an intermediate species formed in gas phase. The formation of the intermediate species is controlled by the decomposition of  $\text{NH}_3$ . At a substrate temperature of 350°C, the deposition rate is controlled by the amount of the intermediate species with higher mass (amu 77,  $\text{Si}_2\text{NH}_6$ ), and the films are polymeric solids. At 500°C, chemical species are deposited on the surface before they grow into the intermediate species with the high mass (amu 77), and the film structure becomes stoichiometric  $\text{SiN}_x$ .

## Introduction

Silicon nitride ( $\text{SiN}_x$ ) films, usually deposited using  $\text{SiH}_4$  and  $\text{NH}_3$ , are widely used in microelectronics. Films deposited by plasma-assisted chemical vapor deposition (plasma-CVD) are applied to a passivating coating and a diffusion barrier, and those by thermal CVD to metal-nitride-oxide-semiconductor (MNOS) memory. In recent years,  $\text{SiN}_x$  deposited at low temperatures by plasma-CVD is adopted to a gate insulator in amorphous thin film transistors. It has been also studied as metal-insulator-semiconductor (MIS) structures of III-V semiconductors.<sup>1-3</sup> For the deposition on crystalline silicon, bombardment by charged particles on the surface of a growing film produces inferior electrical properties such as a low resistivity<sup>4,5</sup> and a large density of states at the interface of an MIS structure.<sup>6,7</sup> Although a higher dielectric constant of  $\text{SiN}_x$  than that of  $\text{SiO}_2$  has been promised in the course of reducing the dimension of microelectronic devices, the use of  $\text{SiN}_x$  is limited.

Photoassisted chemical vapor deposition (photo-CVD),<sup>3,8-11</sup> as well as remote plasma-CVD,<sup>1,12</sup> is a promising method to deposit  $\text{SiN}_x$  films without bombardment. There are several investigations on the deposition of  $\text{SiN}_x$  by Hg-sensitized photo-CVD<sup>3</sup> and direct photo-CVD without Hg-sensitization using a low-pressure Hg lamp.<sup>9,11,13</sup> An ArF excimer laser,<sup>14</sup> or synchrotron radiation<sup>15</sup> is also used as a light source in direct photo-CVD. In photo-CVD films, the density of interface states and the breakdown field are much improved compared with plasma-CVD films.<sup>9,11,14</sup>

In addition, in plasma CVD for  $\text{SiN}_x$  using  $\text{SiH}_4$  and  $\text{NH}_3$ ,  $\text{SiH}_4$  is more easily decomposed by electron impact than  $\text{NH}_3$ . In fact,  $\text{Si}_2\text{H}_6$  is formed in the gas phase with a low

power or a low  $\text{NH}_3/\text{SiH}_4$  gas composition.  $\text{Si}_2\text{H}_6$  is easily decomposed, and Si-rich films are formed. When the decomposition of  $\text{NH}_3$  is enhanced by an increase in the power, the formation of  $\text{Si}(\text{NH}_2)_n$  ( $n = 3$  or 4) in gas phase, detected by the mass analysis, resulted in films containing more nitrogen than stoichiometry.<sup>19</sup> The high power input probably leads to an increase of bombardment by charged particles. In thermal-CVD,<sup>16</sup> it is also known that  $\text{SiN}_x$  films often become Si rich. To obtain a stoichiometric film, the flow rate of  $\text{NH}_3$  needs to be more than 100 times larger than that of  $\text{SiH}_4$ .<sup>17</sup>

To enhance the decomposition of  $\text{NH}_3$ , we have investigated photo-CVD for  $\text{SiN}_x$  deposition, in which  $\text{NH}_3$  is predominantly decomposed by photolysis. Very little is known about deposition processes in direct photo-CVD using a low-pressure Hg lamp. The formation schemes of  $\text{Si}_2\text{H}_6$ ,  $\text{Si}_3\text{H}_8$ , and  $\text{SiH}_x(\text{NH}_2)_{x-4}$  in direct photolysis with an ArF excimer laser already have been proposed based on observations by mass spectroscopy.<sup>18</sup> However, since the reaction processes were monitored at room temperature, they are thought to be different from the case with substrate heating. Furthermore, in photolysis using an ArF excimer laser, most of  $\text{NH}_3$  molecules were decomposed owing to the intense excitation.<sup>18</sup> This may lead to a different reaction scheme in photolysis using a low-pressure Hg lamp emitting much less intense light than the excimer laser.

In this paper, we describe the deposition of  $\text{SiN}_x$  films using  $\text{SiH}_4$  and  $\text{NH}_3$  with a low-pressure Hg lamp (185 nm) at low substrate temperatures (<500°C). The deposition mechanism is investigated based on film structures and transient mass spectroscopy. In the photo-CVD,  $\text{NH}_3$  is predominantly decomposed by photolysis.  $\text{SiH}_4$  is decomposed through reactions with  $\text{NH}_2$  and H produced from  $\text{NH}_3$ , indicating that the decomposition of  $\text{SiH}_4$  is controlled by the amount of  $\text{NH}_2$  or H. This brings stoichiometric film composition, high resistivity, and excellent interface properties between  $\text{SiN}_x$  and crystalline Si in a wide range of the

<sup>a</sup> Present address: Shimadzu Corporation, Kyoto, Japan.

<sup>b</sup> Present address: NEC Corporation, Sagamiyama, Kanagawa, Japan.

<sup>c</sup> Present address: Mitsubishi Electric Corporation, Itami, Hyogo, Japan.